JOURNAL OF AIRCRAFT
Vol. 48, No. 4, July–August 2011

Research on Thermal Characteristics of Photovoltaic Array of Stratospheric Airship

Xiaojian Li,* Xiande Fang,† and Qiuming Dai‡
Nanjing University of Aeronautics and Astronautics, 210016 Nanjing, People's Republic of China

DOI: 10.2514/1.C031295

Solar energy is the ideal power choice for high-altitude long-endurance airships. Photovoltaic array and its operation is one of the most critical aspects to the stratospheric airship's design and capabilities, but the research on thermal characteristics of photovoltaic array for the airship's design is rare. This paper develops the thermodynamic models of photovoltaic array and airship, based on which the three-dimensional temperature profile and output power of photovoltaic array are presented, the effects of the latitude, time of the year, wind speed, and insulation on the power output of the photovoltaic array are investigated, and the effects of photovoltaic array on thermal characteristics of the airship are explored. The results indicate that the latitude, time of the year, wind speed, and insulation affect the quantity and distribution of output power of photovoltaic array, and that the photovoltaic array can aggravate the superheat or supercool of the airship, so that the airship's hull requires higher intensity, expandability, and ductibility.

Nomenclature

A	=	area, m^2
a	=	photovoltaic array absorptivity, visible sunlight
c	=	special heat, $J/kg \cdot K$
c_v	=	specific heat capacity at constant volume, $J/kg \cdot K$
D	=	the characteristic length, m
d	=	thickness, m
G	=	incident radiation, W/m^2
Gr	=	Grashof number
h	=	convective heat transfer coefficient, $W/(m^2 \cdot K)$
I	=	incident solar flux absorbed, W/m^2
I_0	=	reference solar flux, $I_0 = 1367$ W/m^2
I_{DN}	=	solar irradiance flux at the altitude, W/m^2
I_{dh}	=	diffuse irradiation flux on a horizontal plane on clear day, W/m^2
J	=	radiosity, W/m^2
k	=	thermal conductivity, $W/(m \cdot K)$
m	=	mass, kg
$\mathbf{n}$	=	normal vector
P_c	=	power output per square meter of the photovoltaic array, W/m^2
Pr	=	Prandtl number
Q_{cond}	=	conductive heat loss to the airship hull, W
Q_{conv}	=	convective heat loss, W
Q_d	=	diffuse irradiation energy absorbed from the sky, W
Q_{DN}	=	direct solar radiation energy absorbed, W
Q_g	=	reflected solar radiation energy absorbed from the Earth, W
Q_{pow}	=	power output of the photovoltaic array, W
Q_r	=	infrared radiation heat loss to the Earth and sky, W
Q_{rg}	=	infrared radiation heat loss to the Earth, W
Q_{rs}	=	infrared radiation heat loss to the sky, W
Q_{rin}	=	radiative heat transfer between a grid and the other parts of the interior surface of the hull, W
Q_{sun_1}	=	solar radiation energy absorbed by the first layer of the photovoltaic array, W
Q_{sun_2}	=	solar radiation energy absorbed by the second layer of the photovoltaic array, W
$Q_{i,j}$	=	conductive heat transfer between the layers i and $i+1$ of photovoltaic array, W
$Q_{3,hull}$	=	conductive heat transfer between the third layer of photovoltaic array and airship hull, W
Re	=	Reynolds number
T	=	temperature, K
T_{ref}	=	photovoltaic array reference temperature, K
T_s	=	sky effective temperature, K
α_p	=	power-temperature coefficient, 4.5%/K
β	=	angle between normal vector of the plane and the unit vector of direct solar radiance, radians
ε	=	photovoltaic array infrared reflectivity
θ	=	tilt angle of the plane, radian
σ	=	Stefan–Boltzmann constant, $5.67E-8$ $W/(m^2 \cdot K^4)$
τ	=	time, s
φ	=	view factor to the Earth
ϕ	=	view factor to the sky
$\phi_{i,j}$	=	angle factor of the grid i to j
ψ	=	solar azimuth, radian
ω	=	solar elevation, radian

Subscripts

a	=	ambient
air	=	air
free	=	free convection
forced	=	forced convection
g	=	Earth
He	=	helium gas
h	=	airship hull
i	=	grid i
in	=	inside of the airship
k	=	grid k
out	=	outside of the airship
p	=	photovoltaic array
1, 2, 3	=	first, second, and third layer, respectively

I. Introduction

AS A high-altitude platform, the stratospheric airship has a great range of performance capability available to be exploited. The

Received 4 November 2010; revision received 5 January 2011; accepted for publication 10 January 2011.

*College of Aerospace Engineering, Department of Man, Machine, and Environment Engineering, 29 Yudao Street; xiaojianli1984@yahoo.com.cn.
†College of Aerospace Engineering, Department of Man, Machine, Environment Engineering, 29 Yudao Street; xd_fang@nuaa.edu.cn.
‡College of Aerospace Engineering, Department of Man, Machine, Environment Engineering, 29 Yudao Street; daiqiumin913@126.com.

main benefits of airship are extended durations, low cost, and recycling. Currently, United States, Japan, and South Korea are the major countries to develop stratospheric airships [1–9]. To operate at high altitudes for extended durations requires a renewable based power system. Low-altitude airships are fuelled by aviation gasoline, high-quality light diesel oil, or aviation kerosene. When fuels burn, thermal energy is converted to mechanical work to power the airship. However, this type of power systems is not adapted for stratospheric airships due to low-density air in the stratosphere and extended durations. Solar energy is the ideal choice for providing power to high-altitude long-endurance airships, and this type of power system is a photovoltaic (PV) array coupled to an energy storage system [4]. During daytime, the PV array converts solar energy into electrical energy by photoelectric and photochemical effects. During night, the energy storage system provides power to the airship.

The PV array is an important component in the airship power system. The efficiency, mass, surface shape, and position of the PV array influence the airship performance, while latitude, time, airship orientation, airship attitude, airship size, and geometry affect the PV array performance. Therefore, the PV array and its operation are critical to the airship design and capabilities. Besides, the PV array has effects on the temperature profile of the airship hull, the "superheat" or "supercool" of airship, the gas temperature, the airship buoyancy force, the thermal stress of the hull, as well as the airship reliability and lifetime.

In the past decade, many investigations have been carried out on the energy system of the high-altitude platform. Aglietti et al. [10,11] calculated the irradiance in the medium/high troposphere and examined the collection of solar energy using a high-altitude aerostatic platform. Choi et al. [12,13] developed a new concept of high-altitude airship (HAA) configuration that uses PV cells or advanced thermoelectric converters. Naito et al. [14] proposed the design and analysis of solar power system for stratospheric platform airship operations. Harada et al. [9] conducted the experiments on thermal characteristics of a 35 meter-long low-altitude airship equipped with PV array, which was developed as a flying test bed for the development of the stratospheric platform power system consisting of solar cells and regenerative fuel cells. Wang et al. [15], Zheng et al. [16], and Shi et al. [17] studied the solar power and power output of the solar cells on the condition that the conversion efficiency of the solar cells is constant. These researches provide a base for airship energy systems. However, PV array thermoelectric properties and its influence on the airship are rarely investigated.

This work develops the thermodynamic models of PV arrays and airships, based on which the numerical simulation is conducted to show 3-D solar radiation and temperature distribution of the array, to investigate the thermal performance of the PV array and to analyze the effects of the latitude, time of the year, wind speed, and insulation on the power output of the PV array and the effect of the PV array on thermal characteristics of an airship.

II. Thermodynamic Model of the Photovoltaic Array of Airships

Thermal environment of the PV array includes solar radiation, infrared radiation from the sky, reflected solar radiation from the Earth, convective heat transfer, and conductive heat transfer between the array and the airship hull. Figure 1 shows schematically the heat transfer of a PV array.

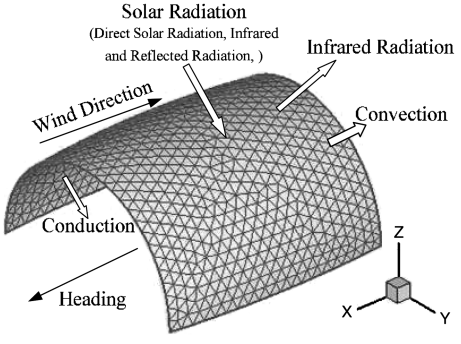

Fig. 1 Schematic diagram of heat transfer of a PV array.

The curved surface of the PV array, which conforms to the airship surface curvature, receives nonuniform solar radiation. A PV array may be divided into n triangular grids, and each grid can be seen as a tilted plane. The heat-balance equation of the grid i may be expressed as

$$m_{p,i}c_p\frac{\mathrm{d}T_{p,i}}{\mathrm{d}\tau}=Q_{\mathrm{sun},i}-Q_{\mathrm{conv},i}-Q_{r,i}-Q_{\mathrm{pow},i}-Q_{\mathrm{cond},i} \quad (1)$$

A. Direct Solar Radiation

The relative position of a grid to the solar radiation is shown in Fig. 2. Assume that the unit vector of direct solar irradiance $\mathbf{E}$ is (e_x, e_y, e_z), where $e_x=\cos\omega\cdot\sin\psi$, $e_y=\cos\omega\cdot\cos\psi$, $e_z=-\sin(\omega)$. The sun elevation and azimuth are defined as

$$\omega=\arcsin(\sin\phi\cdot\sin\delta+\cos\phi\cdot\cos\delta\cdot\cos\varpi) \quad (2)$$

$$\psi=\arcsin(\sin\varpi\cdot\cos\delta/\cos\omega) \quad (3)$$

The (x, y, z) coordinates of the three vertexes of the grid i are $P_1(x_1, y_1, z_1)$, $P_2(x_2, y_2, z_2)$ and $P_3(x_3, y_3, z_3)$, respectively. The normal vector $\mathbf{n}(n_x, n_y, n_z)$ of the grid i is given by

$$\mathbf{n}=\mathbf{P}_1\mathbf{P}_3\times\mathbf{P}_1\mathbf{P}_2=\begin{vmatrix} i & j & k \\ x_3-x_1 & y_3-y_1 & z_3-z_1 \\ x_2-x_1 & y_2-y_1 & z_2-z_1 \end{vmatrix} \quad (4)$$

The tilt angle of the grid i is given by

$$\theta_i=\pi/2+\arcsin\left(\frac{n_z}{\sqrt{n_x^2+n_y^2}}\right) \quad (5)$$

If the grid i faces upward $(n_z>0)$, $\theta_i\in(\pi/2,\pi)$. Otherwise, $\theta_i\in(0,\pi/2)$.

The angle between $\mathbf{E}$ and $\mathbf{n}$ is given by

$$\beta_i=\frac{\mathbf{E}\times\mathbf{n}}{|\mathbf{n}|}=\frac{1}{\sqrt{n_x^2+n_y^2+n_z^2}}\begin{vmatrix} i & j & k \\ e_x & e_y & e_z \\ n_x & n_y & n_z \end{vmatrix} \quad (6)$$

where $\beta_i>\pi/2$ means that the grid i can absorb the solar radiation energy. Otherwise, the grid can not.

B. Absorbed Solar Radiation

The incident solar radiation on the array includes the direct solar radiation, infrared radiation from the sky and reflected solar radiation from the Earth. The absorbed direct solar radiation energy is given by

$$Q_{\mathrm{DN},i}=\alpha A_{p,i}I_{\mathrm{DN}}\sin\omega\cdot\cos(\pi-\beta_i) \quad (7)$$

The absorbed infrared solar radiation energy from the sky is given by

$$Q_{d,i}=\alpha A_{p,i}I_{\mathrm{dh}}(1+\cos\theta_i)/2 \quad (8)$$

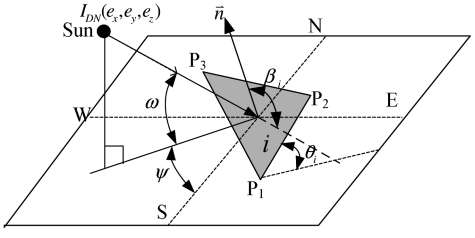

Fig. 2 Direct Solar Radiation Model.

The absorbed reflected solar radiation energy from Earth is given by

$$Q_{g,i} = \alpha A_{p,i}(I_{\mathrm{DN}} \sin\omega + I_{\mathrm{dh}}) \cdot (1 - \cos\theta_i)/2 \tag{9}$$

Summarizing the Eqs. (7–9), the absorbed solar radiation can be expressed as

$$Q_{\mathrm{sun},i} = Q_{\mathrm{DN},i} + Q_{d,i} + Q_{g,i} \tag{10}$$

C. Infrared Radiation Heat Loss

The infrared radiation heat loss of gird i is given by

$$Q_{r,i} = \varepsilon A_{p,i}\sigma[(T_{p,i}^4 - T_s^4)\phi_i + (T_{p,i}^4 - T_g^4)\varphi_i] \tag{11}$$

where the first term on the right hand is the heat loss to the sky and the second to the Earth.

D. Convection Heat Loss

The array surface is exposed to ambient air. Convection of wind over the array can be free or forced. The convection heat loss is given by

$$Q_{\mathrm{conv},i} = A_{p,i}h_{\mathrm{out}}(T_{p,i} - T_a) \tag{12}$$

where the convection heat transfer coefficient in the present study is given by Rapert [18]. For free convection heat transfer:

$$h_{\mathrm{free}} = \frac{k_{\mathrm{air}}}{D}\left\{0.6 + 0.387 \cdot \left[\frac{Gr_{\mathrm{air}}Pr_{\mathrm{air}}}{[1 + (0.559/Pr_{\mathrm{air}})^{9/16}]^{16/9}}\right]^{1/6}\right\}^2 \tag{13}$$

and for force convection between the array and ambient air

$$h_{\mathrm{forced}} = \frac{k_{\mathrm{air}}}{D}Re_{\mathrm{air}}Pr_{\mathrm{air}}[0.2275/(\lg Re_{\mathrm{air}})^{2.584} - 850/Re_{\mathrm{air}}] \tag{14}$$

E. Conductive Heat Loss

The array conforms to the airship surface curvature. If there is no insulation between the array and the airship hull, the remarkable conductive heat transfer to the airship hull from the array exists. The conductive heat loss is given by

$$Q_{\mathrm{cond},i} = A_{p,i}(T_{p,i} - T_h)/(d_p/k_p + d_h/k_h) \tag{15}$$

F. Power Output of the PV Array

The power output of the PV array is determined by the incident solar radiation on the array and the performance characteristics and the geometry of the array. Assuming that the output depends linearly on the incident solar radiation and decreases with temperature, the output of the grid i can be expressed as [19]

$$Q_{\mathrm{pow},i} = A_{p,i}(I_i/I_0)P_c[1 - \alpha_p(T_{p,i} - T_{\mathrm{ref}})] \tag{16}$$

G. Structure Model of the PV Array

The array is composed of glass, encapsulants, solar cells, and substrates, which can be treated as a multilayer model. Thermodynamic properties of each layer are different, and solar radiation absorbed on various parts of the array is nonuniform. The array also can be treated as heat conductor with nonuniform inner heat source. Therefore, a separate heat-balance equation may be written for each layer to obtain a better estimation of the solar cell temperature.

The array may be divided into three layers, which are the cover glass, the solar cells, and the substrate. The first layer (the cover glass) transmits most of the solar flux to the second layer (solar cells). A large portion of solar flux is absorbed by the solar cells and another part is reflected back to the atmosphere through the first layer. The first layer has convective heat transfer with the atmosphere. The third layer has conductive heat transfer with the airship hull. Each layer has conductive heat transfer with the adjacent layer. The mechanism of heat transfer of the array is shown in Fig. 3 and is given by the following three differential time-dependent equations:

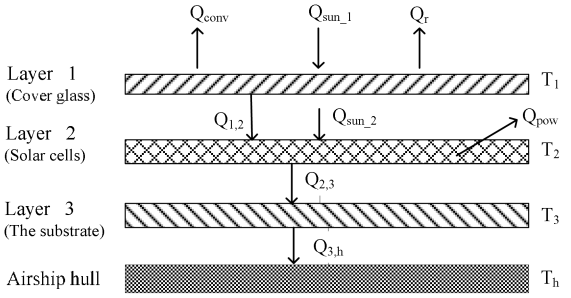

Fig. 3 Heat transfer mechanism of the PV array.

$$m_{p1}c_{p1}\frac{\mathrm{d}T_1}{\mathrm{d}\tau} = Q_{\mathrm{sun}_1} - Q_{\mathrm{co}} - Q_r - Q_{1,2} \tag{17}$$

$$m_{p2}c_{p2}\frac{\mathrm{d}T_2}{\mathrm{d}\tau} = Q_{\mathrm{sun}_2} - Q_{\mathrm{pow}} + Q_{1,2} - Q_{2,3} \tag{18}$$

$$m_{p3}c_{p3}\frac{\mathrm{d}T_3}{\mathrm{d}\tau} = Q_{2,3} - Q_{3,h} \tag{19}$$

where

$$Q_{i,i+1} = A_p(T_i - T_{i+1})/(d_i/k_i + d_{i+1}/k_{i+1}) \tag{20}$$

$$Q_{3,h} = A_p(T_3 - T_h)/(d_3/k_3 + d_h/k_h) \tag{21}$$

III. Thermodynamic Model of Stratospheric Airships

The airship hull is made of laminated membrane materials that are able to support higher inner pressure and to keep buoyant gas inside the hull. Because the hull is thin, the heat conduction of the hull is neglected for the purpose of simplification. The airship is full of buoyant gas, generally helium. Suppose that the hull remains unchanged, and that the different pressure between the buoyant gas and the ambient atmosphere is in the permitted range. Figure 4 is schematic diagram of airship heat transfer.

Various parts of the airship hull receive nonuniform solar radiation. It is desirable to divide the airship hull into small grids, as did for the array. Consequently, the airship hull is treated as a close system consisting of n pieces of isothermal gray-body surface. The heat-balance equation of the grid i of the airship hull may be expressed as

$$m_{h,i}c_h\frac{\mathrm{d}T_{h,i}}{\mathrm{d}\tau} = Q_{\mathrm{sun},i} + Q_{\mathrm{cond},i} - Q_{\mathrm{conv},i} - Q_{r,i} - Q_{\mathrm{cin},i} - Q_{\mathrm{rin},i} \tag{22}$$

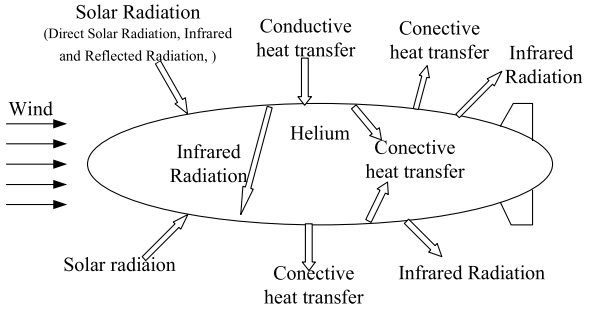

Fig. 4 Schematic diagram of airship heat transfer.

The heat-balance equation of the buoyant gas may be expressed as

$$c_{v,\mathrm{he}} m_{\mathrm{he}} \frac{\mathrm{d}T_{\mathrm{he}}}{\mathrm{d}\tau} = \sum_{i=1}^{N} Q_{\mathrm{cin},i} \tag{23}$$

The internal free convective heat transfer between the buoyant gas and the grid is given by

$$Q_{\mathrm{cin},i} = h_{\mathrm{in}} A_{h,i} (T_{h,i} - T_{\mathrm{he}}) \tag{24}$$

where

$$h_{\mathrm{in}} = 0.13 \frac{k_{\mathrm{He}}}{D} \cdot (Gr_{\mathrm{He}} \cdot Pr_{\mathrm{He}})^{1/3} \tag{25}$$

The radiative heat transfer between the grid i and the other parts of the interior surface of the hull is given by

$$Q_{\mathrm{rin},i} = (J_i - G_i) A_{h,i} \tag{26}$$

where

$$J_i = \varepsilon \sigma T_{h,i}^4 + (1-\varepsilon) \sum_{k=1}^{n} J_k \phi_{i,k} \qquad (k = 1, 2, \cdots, n) \tag{27}$$

$$G_i = (J_i - \varepsilon \sigma T_{h,i}^4)/(1-\varepsilon) \tag{28}$$

Equation (27) can be transformed into

$$\sigma T_{h,i}^4 = \sum_{k=1}^{n} \frac{\delta_{i,k} - (1-\varepsilon)\phi_{i,k}}{\varepsilon} J_k = \sum_{k=1}^{n} a_{i,k} J_k \tag{29}$$

where

$$a_{i,k} = \frac{\delta_{i,k} - (1-\varepsilon)\phi_{i,k}}{\varepsilon} \tag{30}$$

$$\delta_{i,k} = \begin{cases} 1 & k = i \\ 0 & k \neq i \end{cases} \tag{31}$$

Equation (29) can be expressed as

$$\begin{bmatrix} a_{1,1} & a_{1,2} & a_{1,3} & \cdots & a_{1,n} \\ a_{2,1} & a_{2,2} & a_{2,3} & \cdots & a_{2,n} \\ a_{3,1} & a_{3,2} & a_{3,3} & \cdots & a_{3,n} \\ \vdots & \vdots & \vdots & \vdots & \\ a_{n,1} & a_{n,2} & a_{n,3} & \cdots & a_{n,n} \end{bmatrix} \cdot \begin{bmatrix} J_1 \\ J_2 \\ J_3 \\ \vdots \\ J_n \end{bmatrix} = \sigma \begin{bmatrix} T_{h,1}^4 \\ T_{h,2}^4 \\ T_{h,3}^4 \\ \vdots \\ T_{h,n}^4 \end{bmatrix} \tag{32}$$

IV. Numerical Calculation and Analysis

To investigate the thermal performances of the array and the stratospheric airship, the design parameters of the array and the airship listed in Tables 1 and 2 were chosen. The area of the PV array is 620 m^2.

Table 1 Design index of the array [19]

Photovoltaic array layers	Cover glass	Solar cells	Substrate
Absorptivity	0.24	0.64	0.28
Emissivity	0.86	——	0.86
Thermal conductivity, $W/(m \cdot K)$	0.66	137.95	0.4
Specific heat capacity, $J/(Kg \cdot K)$	824	476	1506
Density, kg/m^3	2400	2850	1580
Thickness, mm	0.2	0.33	0.089

Table 2 Design index of the airship

Parameter	Value
Length, m	60
Diameter, m	20
Area, m^2	3000
Volume, m^3	12000
Ceiling altitude, km	20
Longitude and latitude	30°N, 120°E
Absorptivity	0.38
Emissivity	0.86
Buoyant gas	Helium gas
Date	21 June 2009

During daytime, a part of solar energy absorbed on the array converts to electrical energy, while a large portion converts to heat energy. Therefore, the temperature of the array increases. Figure 5 shows 3-D solar radiation and temperature distribution of solar cells at noon. Since the solar radiation on the array is nonuniform, the temperature of the array is nonuniform. The temperature nonlinearly varies with the absorbed solar radiation. The temperature at the top of the array is over 70 K higher than at the bottom at noon, while the temperature difference between the layers of a grid is small due to the small thickness and heat resistence. Normally, three layers may be treated as an isothermal body in thermal analysis.

The power output of the array is determined by the incident solar radiation on the array and the operating temperature of the array, which is directly proportional to the incident solar radiation and inversely proportional to the operating temperature. Figure 6 shows the output profile of the array. During daytime, the output increases firstly reaches its maximum at noon, and decreases afterwards. The output is also influenced by the latitude, time during the year, airship orientation, flight attitude, wind speed, and ambient temperature. The latitude, time during the year, airship orientation, and flight attitude directly influence the incident solar radiation on the array, and flight altitude, wind speed, and ambient temperature affect the convective heat transfer between the array and the atmosphere as well.

Figure 7 shows that flight latitude and time during the year have effects on the output of the array. On 21 June, due to the little incident solar radiation and the low operating temperature of the array, the output at the equator may be more than at the latitude of 30 N at the

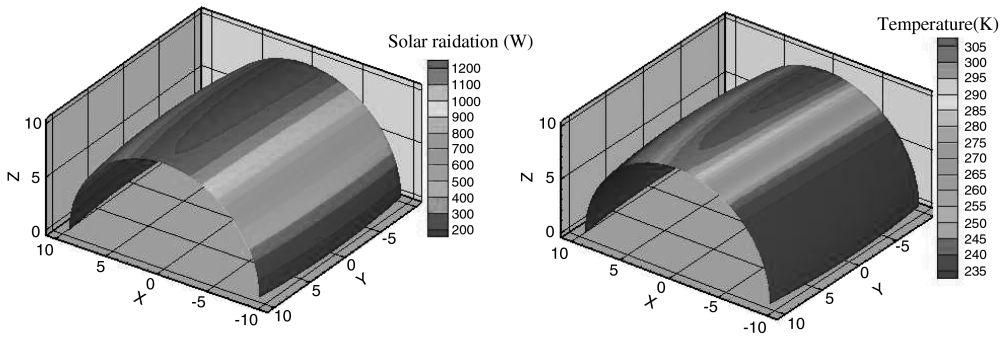

Fig. 5 3-D solar radiation and temperature distribution of solar cells at noon.

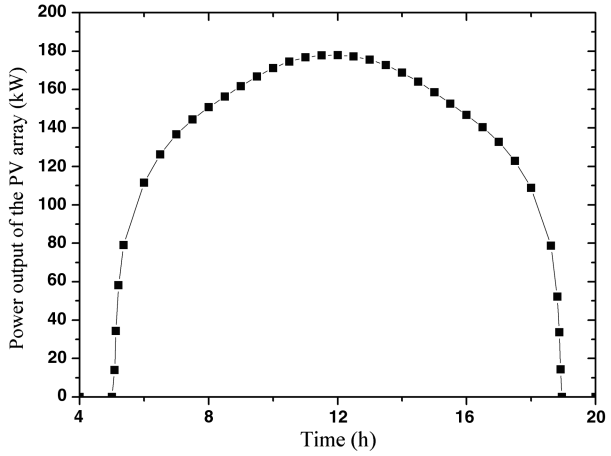

Fig. 6 Power output profile for photovoltaic array.

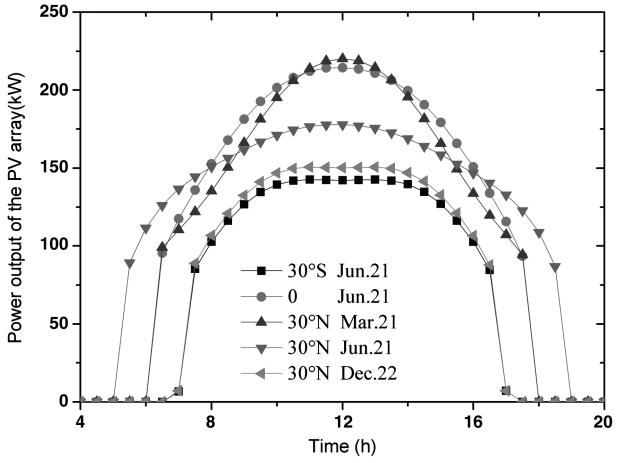

Fig. 7 Effects of latitude and time of the year on power output of photovoltaic array.

same time. Similarly, at the latitude of 30 N, the output on 21 March may be more than that at the same time on 21 June.

Figure 8 shows that the ambient wind speed has effects on the output. The higher the wind velocity is, the more the output of the array will be. As the wind speed increases, the output increases, because convective heat transfer of the outer surface of the array is more intense, and the temperature of the array decreases.

Figure 9 shows that airship orientation has effects on the power output of the array. When the airship orientation changes, the power output of the array varies markedly due to the change of the absorbed

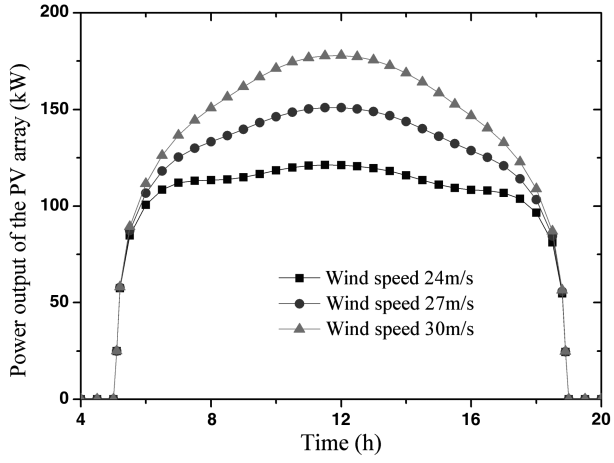

Fig. 8 Effects of wind speed on power output of photovoltaic array.

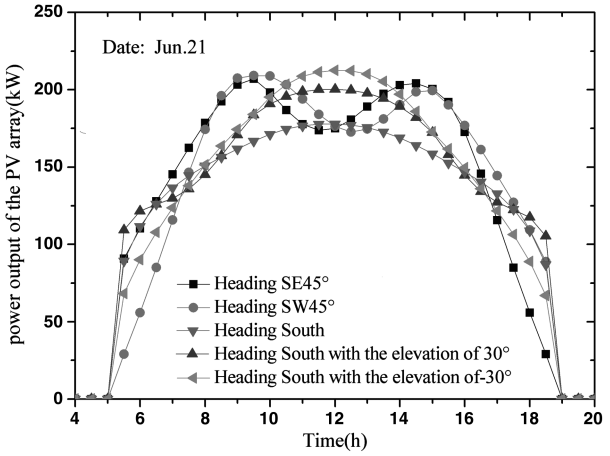

Fig. 9 Effects of airship orientation on power output of photovoltaic array.

solar radiation of the array. Besides, airship size and geometry decide the size and geometry of the array, and thus have effects on the output.

Under the action of the solar radiation, infrared radiation, and convective heat transfer, the airship may "superheat" or "supercool," and the PV array may aggravate the superheat or supercool of the airship. Figures 10 and 11 show temperature distribution of vertical section of the middle part of the airship at noon and at midnight, respectively. During daytime, while the solar radiation is intense, the airship will "superheat." The solar absorptivity of the array is higher than that of the airship hull, so that the local high temperature of the array will aggravate the local superheat of the airship. The bigger the solar absorptivity of the array, the more intense the superheat of the hull. At noon, the temperature at the top of the airship is nearly 310 K with the array, but less than 280 K without the array, about 30 K difference. During night, the temperature of the upper part of the airship hull is lower than the lower part, and thus the upper part is "supercool." It is because the sky effective temperature is lower than the ambient temperature of the airship, and the influence of the infrared radiation between the hull and sky is distinct without the solar radiation. If the emissivity of the array is higher than the airship hull, the supercool of the hull is aggravated. The bigger the emissivity of the array, the more intense the supercool of the hull. In this paper, the emissivity of the array is assumed to be the same as the airship hull, so that the influence of the array on the supercool of the airship hull may be negligible. Besides, the array has an effect on the temperature of the buoyant gas. Figure 12 shows the effect of PV array on the average temperature of helium gas. The PV array may aggravate the variation scope of the temperature and the volume of buoyant gas, so that the airship hull requires higher intensity, expandability, and ductibility.

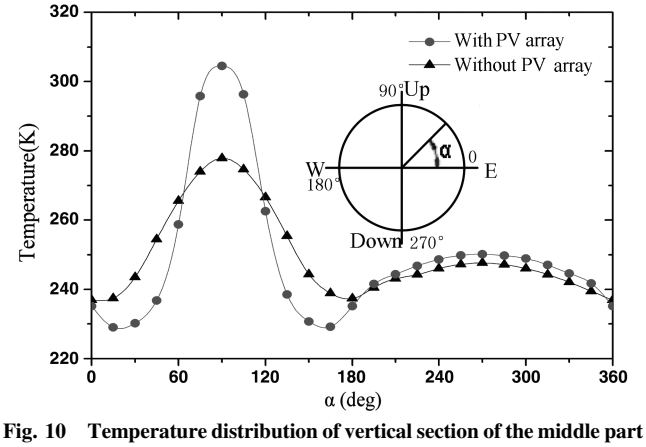

Fig. 10 Temperature distribution of vertical section of the middle part of the airship at noon.

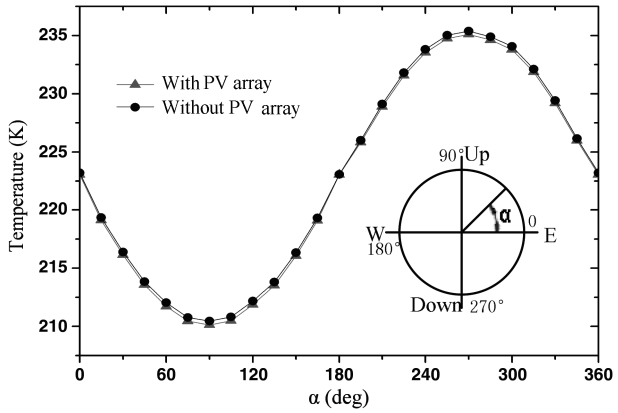

Fig. 11 Temperature distribution of vertical section of the middle part of the airship at midnight.

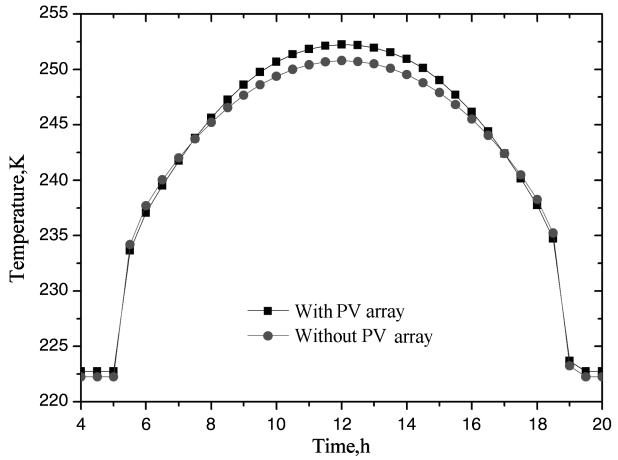

Fig. 12 Effect of photovoltaic array on the average temperature of helium gas.

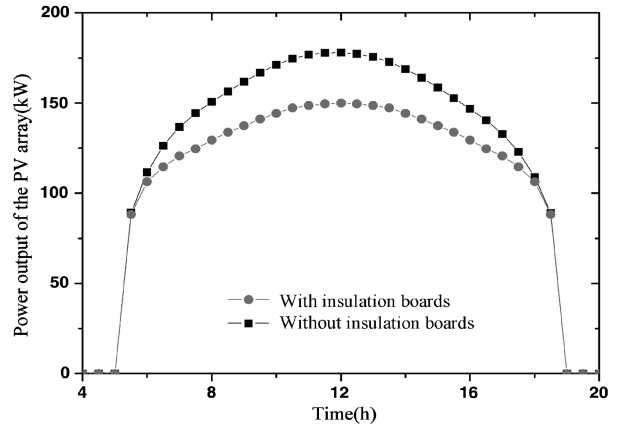

Fig. 13 Effect of insulation on power output of photovoltaic array.

If a thick insulation board is installed between PV array and the airship hull, the superheat of the airship hull and diurnal temperature variation of buoyancy gas can be reduced, which is beneficial for increasing the lifetime of the airship. However, the power output of the array may decrease dramatically (shown in Fig. 13) due to higher operation temperature caused by the insulation. Therefore, the array is more efficient without insulation on its back.

V. Conclusions

The thermodynamic models of the photovoltaic array and airship are developed to estimate the thermal performances of the array, based on which the temperature distribution and power output of the PV array are simulated, the effects of the latitude, wind speed, and insulation on the power output of the PV array are analyzed, and the effect of the PV array on the thermal characteristics of the airship is investigated. The main conclusions are as follows:

1) The temperature distribution of the array is nonuniform due to the incident solar radiation and infrared radiation. The radial temperature difference between the layers is small due to the small thickness and heat resistence. Normally, a three-layer grid of the PV array may be treated as a lumped system to be developed by the lumped method based on heat transfer.

2) The output of the array increases first, reaches its maximum at noon, and decreases afterward. The output may be influenced by various latitudes and the low operating temperature of the array. Besides, the higher the wind velocity is, the more the output of the array will be, due to more intense convective heat transfer and the lower temperature of the array.

3) The PV array may aggravate the superheat or supercool of airship, the variation range of the temperature, and the volume of buoyant gas if there is no insulation between the array and the airship hull. Therefore, the airship hull requires higher intensity, expandability, and ductibility. Insulation installed between the photovoltaic array and the airship hull may reduce the superheat of the airship hull and diurnal temperature variation of buoyancy gas, but the output of the array will decrease.

References

[1] Liao, L., and Pasternak, I., "A Review of Airship Structure Research and Development," *Progress in Aerospace Sciences*, Vol. 45, Nos. 4–5, May–July 2009, pp. 83–96. doi:10.1016/j.paerosci.2009.03.001

[2] Stefan, K., "Thermal Effects on a High Altitude Airship," AIAA Paper A83-38901 17-01, July 1983.

[3] Cathey, H. M., Jr., "Advances in the Thermal Analysis of Scientific Balloons," AIAA Paper 1996-695, Jan. 1996.

[4] Colozza, A., "Initial Feasibility Assessment of a High Altitude Long Endurance Airship," NASA CR-21272, Dec. 2003.

[5] Nachbar, D., and Fabel, J., "Next Generation Thermal Airship," AIAA Paper 2003-6839, Nov. 2003.

[6] Kim, D. M., Lee, Y. G., Kang, W. G., Lee, J.-W., and Yeom, C.-H., "Korea Stratospheric Airship Program and Current Results," AIAA Paper 2003-6782, Nov. 2003.

[7] Lee, Y. G., Kim, D. M., and Yeom, C. H., "Development of Korean High Altitude Platform Systems," *International Journal of Wireless Information Networks*, Vol. 13, No. 1, 2005, pp. 31–42. doi:10.1007/s10776-005-0018-6

[8] Eguchi, K., Yokomaku, Y., and Mori, M., "Feasibility Study Program on Stratospheric Platform Airship Technology in Japan," AIAA Paper 99-3912, Jul. 1999.

[9] Harada, K., Eguchi, K., Sano, M., and Sasa, S., "Experimental Study of Thermal Modeling for Stratospheric Platform Airships," AIAA Paper 2003-6833, Nov. 2003.

[10] Aglietti,G. S., Markvart, T., Tatnall, S. J., and Walker, S. J, "Solar Power Generation Using High Altitude Platforms Feasibility and Viability," *Progress in Photovoltaics: Research and Applications*, Vol. 16, No. 4, 2008, pp. 349–359. doi:10.1002/pip.815

[11] Aglietti, G. S., Markvart, T., Tatnall, A. R., and Walker, S. J, "Aerostat for Electrical Power Generation: Concept Feasibility," *Proceedings of the Institute of Mechanical Engineers, Part G: Journal of Aerospace Engineering*, Vol. 222, No. 1, pp. 29–39. doi:10.1243/09544100JAERO258

[12] Choi, S. H., Elliott, J. R., and King, G. C., "Power Budget Analysis for High Altitude Airships," *Remote Detection Platforms and Technologies, Proceedings of the SPIE*, Vol. 6219, Society of Photo-Optical Instrumentation Engineers, Paper 62190C, May 2006.

[13] Choi, S. H., Elliott, J. R., King, G. C., Park, Y., Kim, J. W., Chu, S. H., and Song, K. D., "Power Technology for Application-Specific Scenarios of High Altitude Airships," *3rd AIAA International Energy Conversion Engineering Conference (IECEC)*, AIAA Paper 2005-5529, Aug. 2005, pp. 15–18.

[14] Naito, H., Eguchi, K., and Hoshino, T., "Design and Analysis of Solar Power System for SPF Airship Operations," *International Balloon Technology Conference*, AIAA Paper 1999-3351, 1999.

[15] Wang, H., Song, B., and Zuo, L., "Effect of High-Altitude Airship's Attitude on Performance of its Energy System," *Journal of Aircraft*, Vol. 44, No. 6, Nov.–Dec. 2007, pp. 2077–2079. doi:10.2514/1.31505

[16] Zheng, W., Song, Q., Li, Y., Wu, Z., and Hu, L., "Computation and Analysis of Power Generated by the Solar Cell Array of a Stratospheric Airship," *Journal of Astronautics*, Vol. 31, No. 4, April 2010, pp. 1224–1230 (in Chinese).

[17] Shi, H., Song, B., and Yao, Q., "Study of the Solar Power System of Stratospheric Airships," *Chinese Space Science and Technology*, Vol. 1, No. , Dec. 2008, pp. 26–31 (in Chinese).

[18] Rapert, C. R. M., "A Heat Transfer Model for a Hot Helium Airship," *7th AIAA Lighter-than-Air Technology Conference*, AIAA Paper 1987-2443, Aug. 1987.

[19] Matz, E., Appelbaum, J., Taitel, Y., and Flood, D. J., "Solar Cell Temperature on Mars," *Journal of Propulsion and Power*, Vol. 14, No. 1, Jan.–Feb. 1998, pp. 119–125. doi:10.2514/2.5257